Polar Meteorol. Glaciol., **18**, 30–53, 2004

Seasonal variation of moisture transport in polar regions and the relation with annular modes

Kazuhiro Oshima* and Koji Yamazaki

Graduate School of Environmental Earth Science, Hokkaido University, Sapporo 060-0810
**Corresponding author. E-mail: kaz@ees.hokudai.ac.jp*

(Received February 5, 2004; Accepted July 16, 2004)

Abstract: Climatological seasonal variations of moisture transport and the inter-annual variations associated with the annular modes in the Arctic and Antarctic regions are investigated using 15-year ECMWF reanalysis data. Over the Arctic, there are strong moisture inflows from the Atlantic and Pacific in all seasons. Over the Antarctic, a strong moisture inflow exists around the Antarctic Peninsula in all seasons and another strong inflow exists over the Bellingshausen Sea and the Amundsen Sea in austral autumn and winter. Transient moisture flux is dominant over stationary flux and transient flux variation mainly controls the seasonal variation of precipitation minus evaporation (*P-E*) in both regions. The seasonal variations of *P-E* show a summer maximum in the Arctic and a winter maximum in the Antarctic. It is mainly governed by the seasonal variation of precipitable water variation in the Arctic and transient eddy activity in the Antarctic. The zonal mean poleward and eastward moisture fluxes in high latitudes are positively correlated with annular modes in both regions. Positive polarity of the Arctic Oscillation is associated with enhanced moisture inflow from the Atlantic, while positive polarity of the Antarctic Oscillation is associated with enhanced moisture inflow west of the Antarctic Peninsula.

key words: atmospheric moisture budget, polar regions, annular mode, reanalysis data

1. Introduction

The Arctic and Antarctic regions are moisture flux convergence areas, atmospheric moisture transport is a primary input of water into the regions. The net input of water from the atmosphere to the surface is the difference between precipitation and evaporation (*P-E*). *P-E* is approximately equals the moisture flux convergence over a long period. Furthermore, the moisture transport directly or indirectly affects the snow, sea ice and ice sheet over the regions. Therefore, atmospheric moisture transport is a critical factor for water balance, especially over the polar regions.

There have been some estimates of these quantities over the Arctic and Antarctic. There are two estimation methods for *P-E*; one is an estimate from the atmospheric moisture budget using rawinsonde, objective analysis or satellite data (*e.g.* Peixoto and Oort, 1983, 1992; Bromwich *et al*., 1995; Groves and Francis, 2002a), the other is direct calculation of *P* and *E*. The latter is estimated from rain gauge observations, snow depth measurements (*e.g.* Sellers, 1965; Baumgarner and Reichel, 1975; Giovinetto

and Bull, 1987), objective analysis or model output data (*e.g.* Cullather *et al*., 1998; Bromwich *et al*., 2000). In general, direct observations suffer from local variations of precipitation. Moreover, surface observations are not reliable over the Arctic Ocean and Antarctica, because the observation network is very sparse and accurate measurement is difficult over Antarctica due to the severe climate and snow drift. Giovinetto and Bull (1987) estimated the *P-E* (accumulation) over Antarctica from glaciological data synthesis, but such data can only estimate the annual mean value. Since *P* from objective analysis data is obtained from short-time integration of the forecast model, it suffers from a spin-up problem. Although *P* from a climate model does not have the spin-up problem, it totally depends on the model performance and the performance of many models is not so good in polar regions. Therefore, the moisture budget method is superior to the direct method in the Arctic and Antarctic regions.

On the moisture transport, the distribution of poleward moisture flux across 70°N that contributes to the *P-E* over the region was investigated with rawinsonde data for 1974–1991 by Serreze *et al*. (1995) and a similar study was done for 1973–1995 by Serreze and Barry (2000). These studies discussed the seasonal variation and the distribution of poleward moisture flux across 70°N. Cullather *et al*. (2000) and Bromwich *et al*. (2000) compared estimates from rawinsonde (Historical Arctic Rawinsonde Archive; HARA) with those from reanalysis data (European Centre for Medium-range Weather Forecasts; ECMWF, National Centers for Environmental Prediction and National Center for Atmospheric Research; NCEP-NCAR) and they found that the meridional moisture flux from rawinsonde is smaller than that from reanalysis in boreal summer. However, these studies did not present the horizontal fields of moisture flux and its seasonal variations in detail.

Over the Antarctic, Yamazaki (1992, 1994, 1997), Bromwich *et al*. (1995) and Cullather *et al*. (1998) estimated *P-E* with operational numerical analysis data. Yamazaki (1992, 1994) found that *P-E* is large in austral winter and suggested that it is controlled by cyclone activity. This peculiar seasonal variation was also presented by Bromwich *et al*. (1995). However, the mechanism of this peculiar seasonal variation has not been quantitatively explained yet. Bromwich *et al*. (1995) compared the three operational numerical analyses (ECMWF, National Meteorological Center; NMC, Australian Bureau of Meteorology; ABM) and rawinsonde data, and it was found that the ECMWF analysis provides good estimates for the water budget.

The Arctic Oscillation (AO) is a dominant mode of atmospheric variability in the wintertime Northern Hemisphere (Thompson and Wallace, 1998, 2000). The AO is a seesaw of sea level pressure between the Arctic region and mid-latitudes, which shows an annular pattern. Thus it is also named the Northern Hemisphere Annular Mode (NAM). The Southern Hemisphere counterpart of the AO/NAM is called the Antarctic Oscillation (AAO) or the Southern Hemisphere Annular Mode (SAM) (Gong and Wang, 1999; Thompson and Wallace, 2000). When the phase of the annular mode (AO or AAO) is positive, westerly winds around 60°N/S are enhanced and those around 35°N/S are reduced. Although the annular modes exist throughout the year, they are most active during cold seasons.

Moisture transport is also related to the annular modes (AO and AAO). The zonal mean poleward moisture flux at high-latitudes has a positive correlation with the

AO and AAO (Rogers *et al*., 2001; Boer *et al*., 2001). Although these studies show the zonal mean moisture flux associated with the annular modes, the spatial patterns are not shown. Groves and Francis (2002b) showed composite maps of moisture flux associated with high and low polarities of the AO index. They calculated the moisture flux with moisture data from TOVS and wind data from NCEP-NCAR. Their climatological moisture flux fields are different from those in the present study. There are no studies on the spatial pattern associated with the AAO.

In this study, we examine the seasonal variation of moisture flux fields mainly using the 15-year (1979–1993) ECMWF reanalysis data; the focus is on net moisture inflow into the polar regions. To isolate the effect of cyclone activity on moisture transport, we divide the total moisture transport into transient and stationary components. For the atmospheric moisture budget, most previous studies only presented the *P-E* estimates over the region poleward from 70° (hereafter called the polar cap region), especially in the Arctic. However, to assess the fresh water balance of the Arctic Ocean or the accumulation of moisture in Antarctica, it is useful to examine the moisture budget over the Arctic Ocean or Antarctica. Hence the moisture budget for the Arctic Ocean and Antarctica are also estimated. Interannual variability of moisture transport associated with annular modes is also investigated in this study. In particular, the spatial patterns in both regions are presented.

In Section 2, we describe the data and method used in our analysis. The climatological descriptions of moisture flux and moisture budget in both regions are presented in Section 3. Interannual variability associated with annular modes is presented in Section 4. We summarize with some discussion in Section 5.

2. Data and method

Two reanalysis data sets are used to estimate the moisture flux. The primary data set is the 15-year ECMWF reanalysis (ERA, 1979–1993); the supplementary data set is the 24-year National Centers for Environmental Prediction—Department of Energy (NCEP-DOE) reanalysis-2 (NCEP R2, 1979–2002). Their horizontal resolutions are 2.5 degrees in latitude and longitude in both data sets. Temporal resolution is twice-daily (12 hours) in ERA and fourth-daily (6 hours) in NCEP R2.

Moisture flux $\langle q\mathbf{v}\rangle$ in this paper is a vertical integral of moisture flux $q\mathbf{v}$ at each level and is expressed as follows:

$$\langle q\mathbf{v}\rangle = \frac{1}{g}\int_{300\,\mathrm{hPa}}^{p_{\mathrm{surface}}} q\mathbf{v}\,\mathrm{d}p, \tag{1}$$

where q is the specific humidity, $\mathbf{v}$ is the horizontal wind vector and the brackets represent vertical integration. The upper limit of the integral is set to 300 hPa, because moisture above 300 hPa is negligible.

Monthly mean moisture flux is computed from twice-daily or fourth-daily moisture flux. The monthly mean total moisture flux can be divided into stationary flux and transient flux as follows:

$$\langle \overline{q\mathbf{v}}\rangle = \langle \bar{q}\,\bar{\mathbf{v}}\rangle + \langle \overline{q'\mathbf{v}'}\rangle, \tag{2}$$

where the overbar represents the time average, represented by the monthly average in

this study, and the prime represents the deviation from the time average. Thus total flux (left hand side) is expressed as a sum of stationary (first term of the right hand side) flux and transient (second term of the right hand side) flux. The total flux is obtained from the monthly mean of twice-daily (fourth-daily) flux and the stationary flux is calculated from the monthly mean fields of wind, moisture and surface pressure. The transient flux is calculated by subtracting the stationary flux from the total flux.

To estimate seasonal variations of precipitation minus evaporation (*P-E*) over both the Arctic Ocean and Antarctica, we define the regions of the Arctic Ocean and Antarctica with ERA land-sea mask data (Fig. 1). *P-E* is estimated by the atmospheric moisture budget equation as follows:

$$\frac{\partial PW}{\partial t} = -\nabla\langle q\mathbf{v}\rangle + E - P, \tag{3}$$

where PW is precipitable water. When we calculate an average over a long time period (*i.e.*, seasonal mean), the time rate of change of PW, the left hand side of eq. (3), can be neglected and eq. (3) is rewritten as:

$$\begin{aligned} P - E &\approx -\nabla\langle q\mathbf{v}\rangle \\ &\approx -\frac{1}{A}\oint \langle q\mathbf{v}\rangle \cdot \mathbf{n}\, dl, \end{aligned} \tag{4}$$

where A is the area of the region, l is the length along the boundary of the region and $\mathbf{n}$ is the unit vector normal to the boundary of the region.

To clarify the relation between annular modes and moisture flux, the correlation coefficients between Arctic and Antarctic Oscillation indices and zonal mean moisture flux are calculated based on 15-year monthly mean data. Prior to the analysis, climatological seasonal variation of moisture flux is removed from the moisture flux data. We show the regression patterns for moisture flux upon the AO/AAO indices.

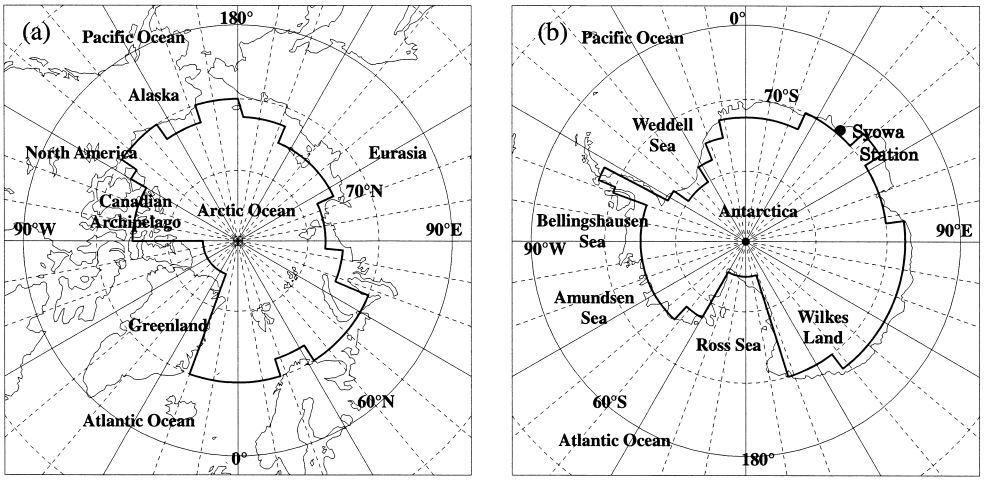

Fig. 1. Maps of (a) the Arctic region and (b) the Antarctic region. Bold solid lines indicate the boundaries of the Arctic Ocean and Antarctic regions used to estimate "Precipitation minus Evaporation" (P-E) in this study.

The monthly mean AO and AAO indices available at NOAA Climate Prediction Center are used.

3. Climatology of atmospheric moisture transport and budget

3.1. The Arctic

3.1.1. Annual mean field

Climatological fields of annual mean moisture flux and precipitable water (PW) in the Northern Hemisphere are shown in Fig. 2a. Northeastward moisture fluxes are strong over the Pacific and Atlantic Oceans in mid-latitudes, corresponding to the dominant storm track over each region. PW decreases with latitude, and with altitude of topography.

Figure 2b is the same as in Fig. 2a but for poleward from 60°N (the Arctic region). Over the Arctic, there are strong moisture inflows from the Atlantic Ocean and the Pacific Ocean. It is also clear that moisture is transported eastward from the Atlantic Ocean to the interior of Siberia and from the Pacific Ocean to the interior of North America. These moisture fluxes are related to the mean wind in the lower troposphere. At the same latitudes, PW is large in the Atlantic sector (30°W–20°E) because of moisture transport from low latitudes over the warm Atlantic Ocean.

Annual mean stationary and transient moisture fluxes are shown in Figs. 3a and 3b, respectively (the corresponding total flux is shown in Fig. 2b). The stationary flux field is similar to the total flux field, but the stationary flux shows small inflows from the Atlantic and Pacific Oceans and large outflow through the Canadian Arctic Archipelago. On the other hand, transient fluxes are poleward at all longitudes and they are strong in the Atlantic and the Pacific sectors (180°–15°W). Inflow can be seen on the western side of Greenland and in Eastern Europe (45°E–90°E). Even over the Canadian Arctic Archipelago, where the stationary flux shows large outflow from the Arctic, the transient flux indicates inflow to the Arctic Ocean. In general, poleward flow ($v' > 0$) is accompanied with more humid air ($q' > 0$) while equator-ward flow ($v' < 0$) is accompanied with drier air ($q' < 0$). Therefore, the correlation between q' and v' is positive in the Northern Hemisphere. Thus, transient eddies, typically associated with extratropical cyclones, transport moisture poleward.

3.1.2. Seasonal variation of moisture flux

Figure 4 presents the seasonal mean moisture flux and PW fields over the Arctic. There are primary moisture inflow from the Atlantic Ocean and secondary moisture inflow from the Pacific Ocean in all seasons, as seen in the annual mean field (Fig. 2b). The flux pattern in summer (JJA) is different from that in other seasons. In summer, moisture fluxes are strong due to summer moisture abundance. The PW over the Arctic Ocean in summer is about five times larger than that in winter (Figs. 4a, c). The inflow from the Pacific to the Arctic Ocean through Alaska is largely enhanced, but the subsequent outflow through the Canadian Arctic Archipelago is also enhanced. Cyclonic flow also appears over the Arctic Ocean. These flows are seen in wind fields in the lower troposphere. These inflows and outflows correspond to the mean wind. On the other hand, in other seasons (DJF, MAM, SON), moisture is transported eastward from the Atlantic Ocean to the interior of Siberia and from the Pacific Ocean

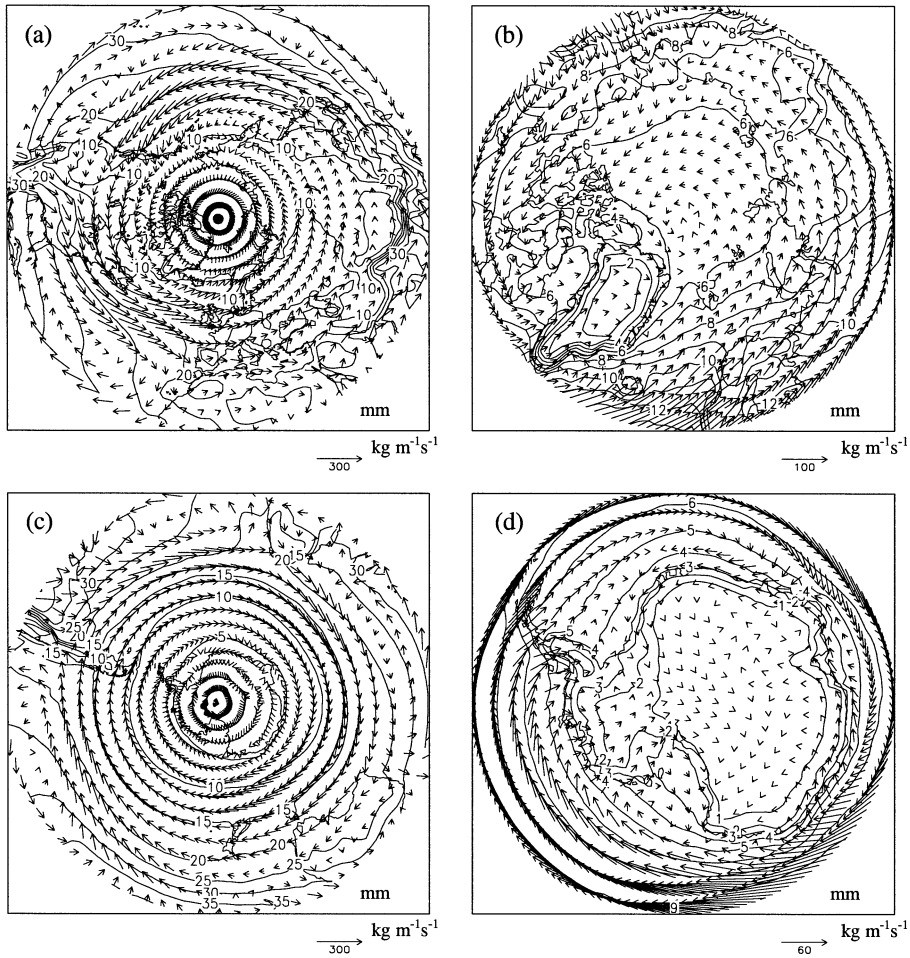

Fig. 2. Climatological fields of annual mean moisture flux and precipitable water (PW). The 15-year (1979–1993) ECMWF reanalysis data are used. (a) The Northern Hemisphere (north of 20°N), (b) the Arctic (north of 60°N), (c) the Southern Hemisphere (south of 20°S), and (d) the Antarctic (south of 60°S). Vectors denote moisture flux and contours denote PW. The arrow scale for moisture flux is shown at the bottom of each panel. Note that the arrow scales are different among maps. The contour intervals in (a) and (c) are 5 mm, and those in (b) and (d) are 1 mm.

and Alaska to the interior of North America. In winter (DJF), the wind field shows a cross-Arctic flow in the Arctic Ocean, but such a flow is not seen in the moisture flux (Fig. 4a) due to small *PW* in this season.

Stationary and transient flux fields in winter (DJF) and summer (JJA) are shown in Fig. 5. In winter, the stationary flux pattern is similar to the total flux pattern, but the inflows from the Atlantic Ocean and the Pacific Ocean are weaker than the total flux fields. Transient fluxes are large in these regions and transient components make inflows stronger. Similar characteristics are seen in summer. In summer, moreover,

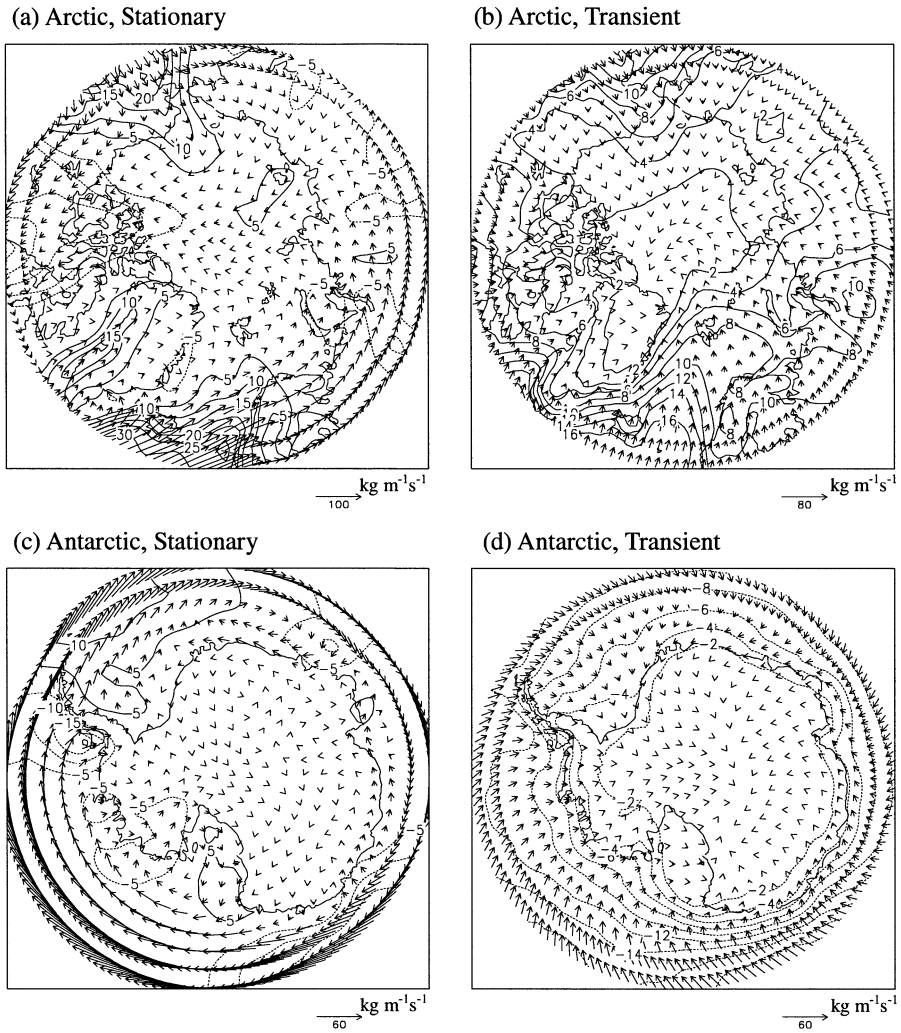

Fig. 3. Climatological fields of the annual mean stationary and transient components of moisture flux. The 15-year (1979–1993) ECMWF reanalysis data are used. The stationary flux is calculated from the monthly mean fields of wind, moisture and surface pressure. The total flux is obtained from the monthly mean of twice-daily flux, which is shown in Fig. 2. The transient flux is calculated by subtracting the stationary flux from the total flux. (a) Stationary moisture flux in the Arctic, (b) transient moisture flux in the Arctic, (c) stationary moisture flux in the Antarctic, and (d) transient moisture flux in the Antarctic. Vectors denote moisture flux and contours show their northward components. The arrow scale for moisture flux is shown at the bottom of each panel. Note that arrow scales are different among maps. The contour intervals in (a) and (c) are 5 kg m^{-1}s^{-1}, and those in (b) and (d) are 2 kg m^{-1}s^{-1}.

there is strong inflow in Central Eurasia (around 90°E) due to transient flux. The outflow through the Canadian Archipelago is large in the stationary and weak in the total component. As described above, since the transient flux is generally poleward,

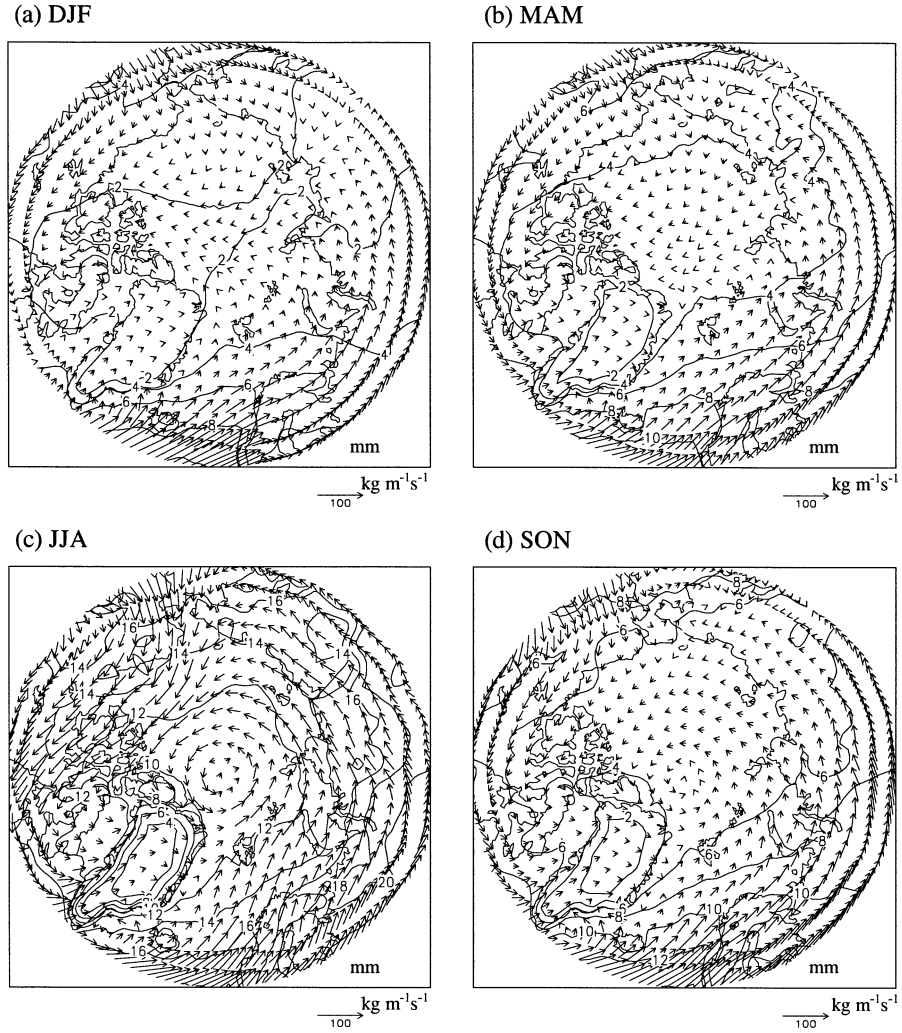

Fig. 4. Seasonal mean climatological fields of moisture flux and precipitable water (PW) for the Arctic. The 15-year (1979–1993) ECMWF reanalysis data are used. (a) Winter (December, January and February), (b) spring (March, April and May), (c) summer (June, July and August), and (d) autumn (September, October and November). Vectors denote moisture flux and contours PW. The arrow scale for moisture flux is shown at the bottom of each panel. Contour interval is 2 mm in all maps.

inflow becomes strong and outflow becomes weak in total flux fields.

3.1.3. Moisture budget in the Arctic region

To examine the seasonal variation of poleward moisture flux more clearly, monthly mean northward moisture flux across 70°N is shown in Fig. 6. There is poleward moisture flux at most longitudes throughout the year. The inflow and outflow are enhanced in summer, especially in July and August. In the Atlantic sector (20°W–30°E), the poleward moisture flux can be seen throughout the year; it shows semi-annual

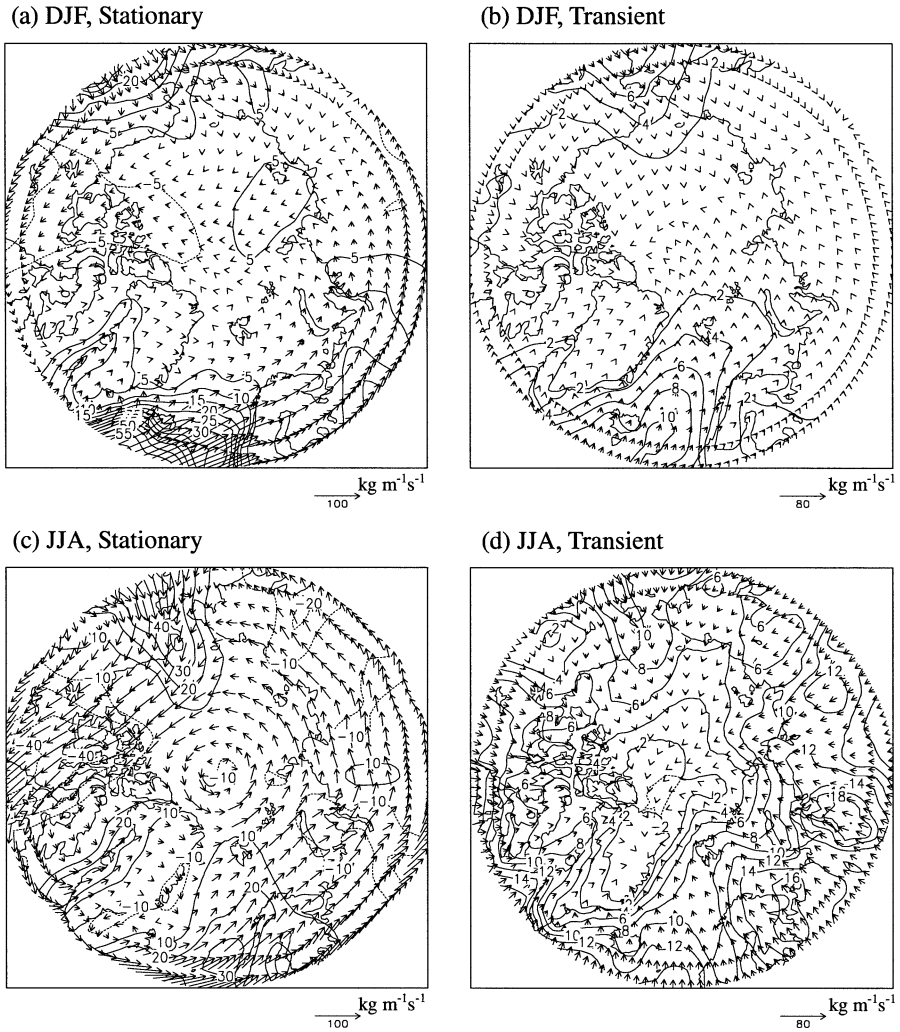

Fig. 5. Climatological fields of stationary and transient components of moisture flux over the Arctic for winter (December, January and February) and summer (June, July and August) seasons. The 15-year (1979–1993) ECMWF reanalysis data is used. The calculation method of stationary and transient components is the same as that in Fig. 3. (a) Stationary moisture flux in winter, (b) transient moisture flux in winter, (c) stationary moisture flux in summer, and (d) transient moisture flux in summer. Vectors denote moisture flux and contours show their northward components. The arrow scale for moisture flux is shown at the bottom of each panel. Note that arrow scales are different among maps. The contour interval in (a) is 5 kg m^{-1} s^{-1}, those in (b) and (d) are 2 kg m^{-1} s^{-1}, and that in (c) is 10 kg m^{-1} s^{-1}.

variation in strength with winter and summer peaks. The poleward flux from the Pacific (180°–150°W) shows a strong peak in July, accompanied by a strong peak of equator-ward flux through the Canadian Arctic Archipelago (120°–90°W). There are also enhanced poleward fluxes in summer around west Siberia (80°–100°E) and west of

Greenland (50°W). These two inflows show maxima in August. These fluxes contribute to the moisture flux convergence over the Arctic region.

The seasonal variations of *P-E* over the Arctic Ocean calculated from stationary

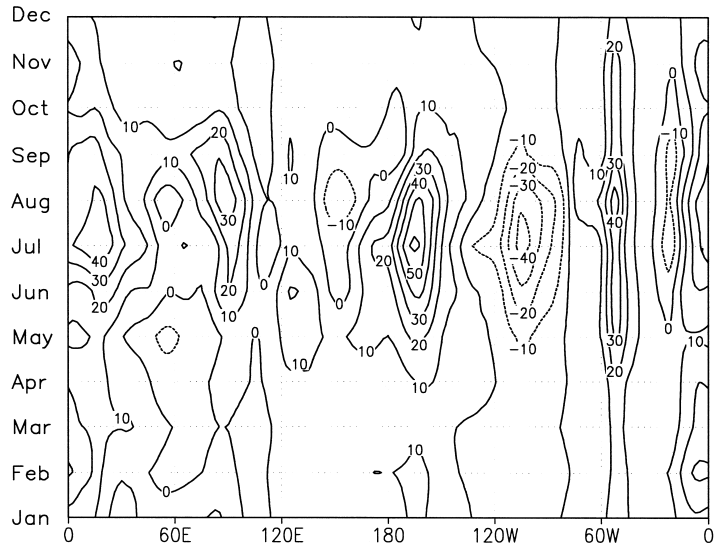

Fig. 6. Seasonal variation of northward moisture flux at 70°N. The 15-year (1979–1993) ECMWF reanalysis data are used. Contour interval is 10 kg m^{-1} s^{-1}.

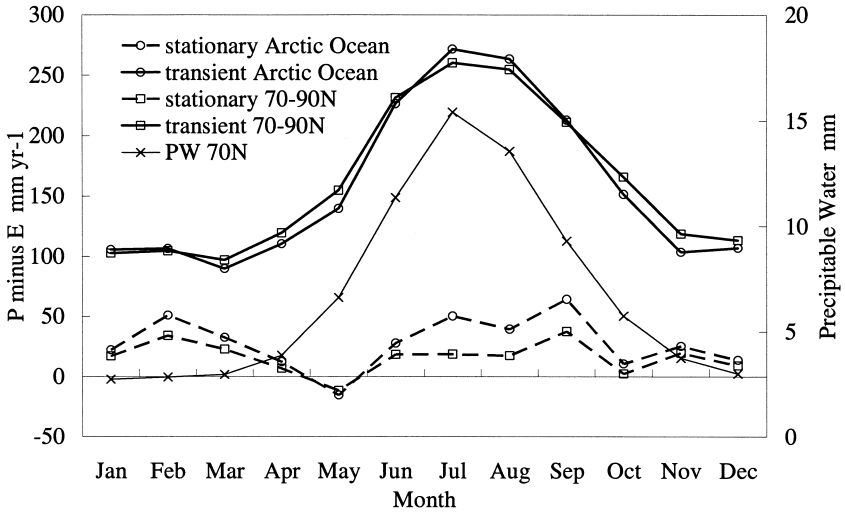

Fig. 7. Seasonal variations of "Precipitation minus Evaporation" (P-E) estimated from stationary and transient components of moisture flux. Bold solid lines indicate the P-E estimate from the stationary component of moisture flux and dashed lines are the estimate from the transient component. "Circles" (○) and "Squares" (□) denote the region of the Arctic Ocean (the region shown in Fig. 1) and the region north of 70°N, respectively. "Crosses" (×) denote zonal mean precipitable water (PW) at 70°N. The scale of PW is shown at the right side of the figure.

and transient moisture fluxes are presented in Fig. 7. The *P-E* from the transient flux is much larger than that from the stationary flux throughout the year. The amplitude of seasonal variation from the transient flux is larger than that from the stationary flux. Therefore, the seasonal cycle of *P-E* over the Arctic is controlled by the transient flux. *P-E* from the transient flux exhibits a summer maximum, even though transient eddy activity of the atmospheric motion itself exhibits a summer minimum. This discrepancy can be explained by a large summer peak in precipitable water (*PW*). The summer maximum of *PW* is five times larger than the winter values. In the Arctic region, the effect of *PW* is dominant over the eddy effect. The *P-E* from stationary flux shows maxima in February and September, for which the reason is unclear.

As in Fig. 7, Fig. 8 shows the seasonal variation of *P-E* over the Arctic Ocean and the north polar cap region (poleward from 70°N) but for the total moisture flux. *P-E* over the Arctic Ocean is large in summer, June to September; it is almost constant in other seasons. The maximum appears in July and the minimum in December. This variation is similar to that over the north polar cap region. The result for the north polar cap region is consistent with previous studies (Cullather *et al.*, 2000; Bromwich

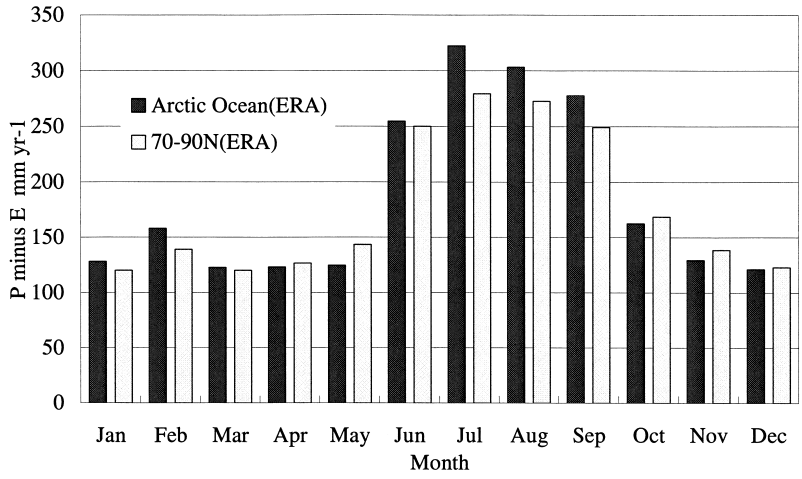

Fig. 8. Seasonal variation of "Precipitation minus Evaporation" (P-E) over the Arctic Ocean (the region shown in Fig. 1, black bar in Fig. 8) and the region poleward of 70°N (gray). The 15-year (1979–1993) ECMWF reanalysis data are used.

Table 1. Seasonal mean and annual mean Precipitation minus Evaporation (P-E) over the Arctic Ocean and Antarctica based on 15-year (1979–1993) ECMWF reanalysis data. Unit is mm yr^{-1}.

	DIF	MAM	JJA	SON	Annual
Arctic Ocean (ERA)	136	123	294	190	186
70°–90°N (ERA)	127	130	267	186	178
Antarctic (ERA)	124	184	197	157	166
70°–90°S (ERA)	99	175	177	149	150

Table 2. Annual mean Precipitation minus Evaporation (P-E) over the Arctic Ocean, compariaon with previous studies. Unit is mm yr^{-1}.

	Arctic Ocean	70–90°N
Based on atmospheric data		
Peixoto and Oort, 1983 (Rawinsonde): 1963–1973	–	116
Serreze and Barry, 2000 (HARA, rawin sonde): 1974–1991	153	161
Groves and Francis, 2002 (TOVS satellite): 1979–1998	145	151
Bromwich *et al*., 2000 (ERA): 1979–1993	179	182
Bromwich *et al*., 2000 (NCEP-NCAR): 1979–1993	194	195
This study (ERA): 1979–1993	186	178
This study (NCEP R2): 1979–2002	198	198
Based on surface data		
Sellers (1965) multiyear	120	50
Baumgartner and Reichel (1975)	44	58

et al., 2000), based on reanalysis data. Seasonal mean *P-E* over the Arctic and the north polar cap region derived from ERA are shown in Table 1. Over the Arctic Ocean, the annual mean *P-E* is 186 mm/year, the summer (JJA) mean is 294 mm/year and the winter (DJF) mean is 136 mm/year. These values over the Arctic Ocean are larger than that over the north polar cap region. This is also seen in Fig. 8. This may be caused by the fact that the north polar cap region includes Greenland and underestimates *P-E* over this region.

Table 2 presents the annual mean *P-E* over the Arctic Ocean, together with results from previous studies. The values of *P-E* over both the Arctic Ocean and the north polar cap in this study are reasonable. The *P-E* from NCEP R2 is a little larger than that from ERA. This is consistent with Cullather *et al*. (2000). Bromwich *et al*. (2000) used the same ERA data set as this study and therefore estimates over the polar cap region are almost the same. However, the estimates over the Arctic Ocean are different, because Bromwich *et al*. (2000) defined a simpler boundary of the Arctic Ocean than that of this study (Fig. 1a). The estimates from surface data vary widely. Those from atmospheric data, especially results from objective analysis data, do not vary widely, but depend on the data set.

3.2. The Antarctic

3.2.1. Annual mean field

In the same way as the Arctic, results for the Antarctic region are shown in this section. In the Southern Hemisphere, annual mean moisture flux and *PW* are zonal in comparison with the Northern Hemisphere and eastward fluxes are strong in mid-latitudes (Fig. 2c). Over the Antarctic, the eastward flux is strong over the Antarctic Ocean surrounding Antarctica. A westward moisture flux exists along the coastline of East Antarctica (Fig. 2d). These transports are related to the mean wind in the lower troposphere. The poleward flux is strong around the Antarctic Peninsula and over the Bellingshausen and the Amundsen Seas. Poleward fluxes also appear off Wilkes Land, and around Syowa Station. This corresponds to the mean wind. These features are consistent with results in Yamazaki (1992, 1994, 1997).

Annual mean stationary and transient flux fields are shown in Figs. 3c and 3d. Stationary fluxes are weaker than total fluxes, but the inflow regions are almost the same. In addition, there are outflows over the Weddell Sea and Ross Sea. Such fluxes are not seen in the total flux field. Transient fluxes are poleward at all latitudes. Thus, inflow of the total component is strong around the Antarctic Peninsula, over the Bellingshausen and Amundsen Seas, off Wilkes Land and around Syowa station. Over the Ross Sea and Weddell Sea, stationary and transient fluxes almost cancel each other and the significant meridional transports over the regions do not appear in the total field.

3.2.2. Seasonal variation of moisture flux

Figure 9 presents the seasonal mean moisture flux and *PW* fields over the Antarctic. There is large eastward flux over the Antarctic Ocean surrounding Antarctica in all seasons. This basically corresponds to the mean wind field in the lower troposphere. The poleward flux is strong around the Antarctic Peninsula. In summer (DJF), the westward moisture flux parallel to the coastline is significantly enhanced in East Antarctica, because the mean low-level wind corresponding to the flux is strong in summer and the *PW* in summer is two times larger than in winter. In autumn (MAM) and winter (JJA), poleward flux is enhanced over the Bellingshausen Sea and the Amundsen Sea.

Stationary and transient fluxes in summer (DJF) and winter (JJA) are shown in Fig. 10. There are similar inflow and outflow patterns in the stationary components in both summer and winter. Due to *PW* increase in summer, the inflow and outflow are strong in summer, especially around the Antarctic Peninsula, off Wilkes Land and around Syowa Station. In the Amundsen Sea, poleward stationary flux is enhanced in summer, which corresponds to the eastern part of the stationary cyclone over the Ross Sea.

Transient poleward flux in winter is generally larger than that in summer even though *PW* is two times larger in summer. This large transient flux indicates that the effect of cyclone activity dominates over the *PW* effect around Antarctica.

3.2.3. Moisture budget in the Antarctic region

Seasonal variation of moisture inflow into the Antarctic at 67.5°S is shown in Fig. 11. We chose 67.5°S instead of 70°S, because the 70°S latitude circle passes through East Antarctica. As in the Arctic, there is poleward moisture flux at most longitudes throughout the year. Note that negative value means poleward flux. There is large poleward flux in summer and small flux in winter around the Antarctic Peninsula (80°–60°W). However, there is large poleward flux in early winter and small flux in summer over the Bellingshausen Sea and the Amundsen Sea (150°–100°W). Large inflow exists around Syowa Station (20°–50°E) in late summer, January to March. A small outflow appears around 60°E throughout the year and in the sector between 45°W and 10°E in late summer.

Figure 12 shows the seasonal variation of *P-E* over Antarctica. This is estimated from stationary and transient moisture fluxes. As in the Arctic region, the *P-E* estimated from transient flux is larger than that from stationary flux. However, the seasonal variation of *P-E* from transient flux is comparable to that from stationary flux. The summer maximum of *PW* over Antarctica is only two times larger than the winter minimum. This explains the peculiar seasonal cycle of *P-E* over Antarctica. In

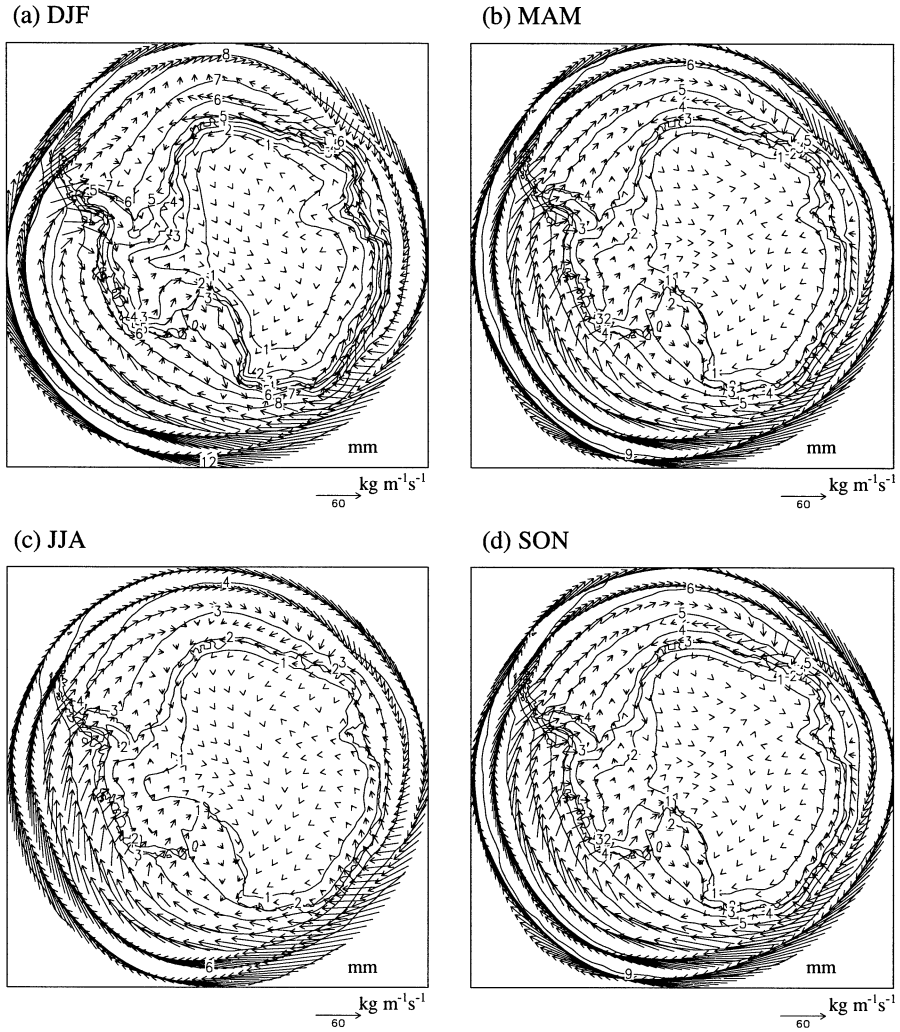

Fig. 9. Same as in Fig. 4 but for the Antarctic. The contour interval is 1 mm in all maps.

Antarctica, the effect of eddy activity dominates over the *PW* effect. The contribution from stationary flux also shows a winter maximum. This is caused by the winter intensification and southern shift of the stationary cyclone in the Ross Sea, which brings humid air poleward to the east of the cyclone (120°W–160°W, see Fig. 10c). Both transient and stationary components contribute to cause this peculiar winter maximum of *P-E* over the Antarctic region.

The seasonal variation of *P-E* over Antarctica and the south polar cap region estimated from total flux is presented in Fig. 13. *P-E* varies gently. In spite of large *PW* in summer and small *PW* in winter, *P-E* is large in winter and small in summer. The maximum appears in July and the minimum in January. This is mainly because transient poleward moisture transport associated with cyclone activity is enhanced in

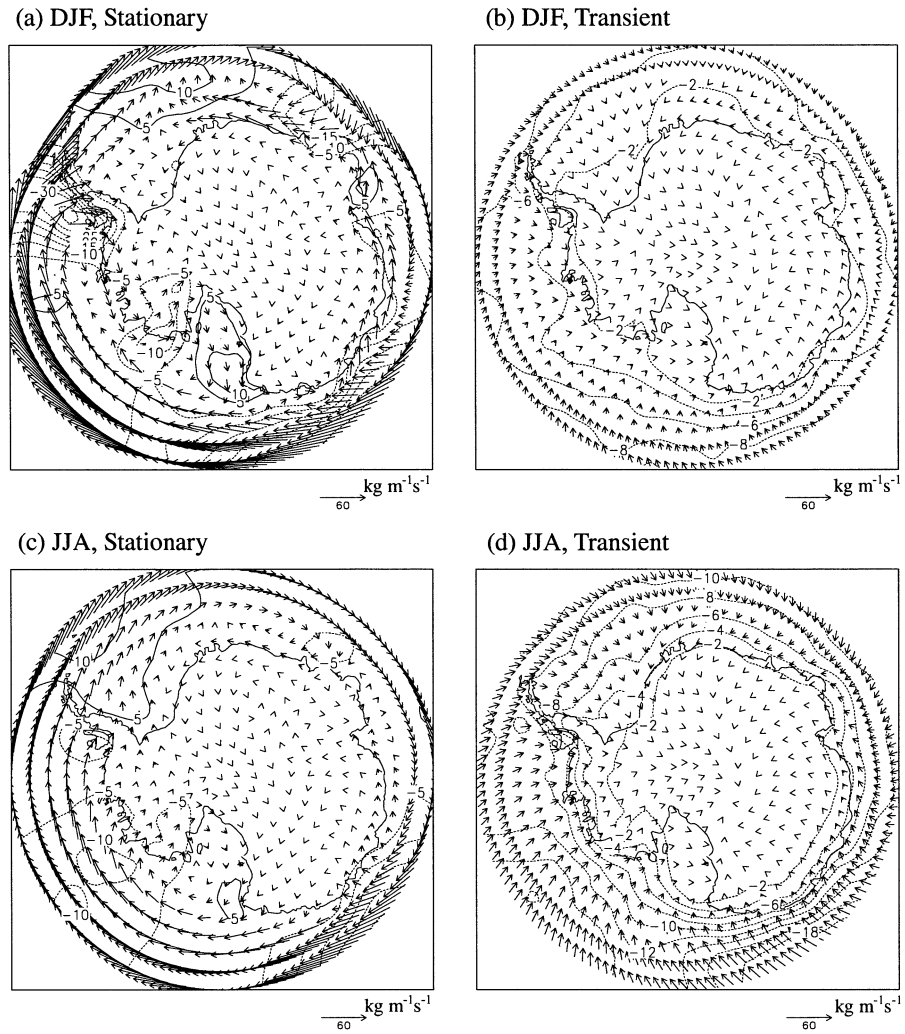

Fig. 10. Same as in Fig. 5 but for the Antarctic. The contour intervals in (a) and (c) are 5 kg m^{-1}s^{-1}, and those in (b) and (d) are 2 kg m^{-1}s^{-1}.

winter (JJA) as seen in Figs. 9, 10 and 12. The stationary flux also contributes to this peculiar seasonal variation. *P-E* over the south polar cap region has a maximum in May and a minimum in January. The present result for Antarctica and the south polar cap region agrees with that of Bromwich *et al.* (1995).

Table 1 shows the seasonal mean *P-E*. Over Antarctica, the annual mean *P-E* is 166 mm/year, the summer (DJF) mean is 124 mm/year and the winter (JJA) mean is 197 mm/year. The seasonal variation in the south polar cap region is slightly larger than that over Antarctica. This is probably because the south polar cap region includes the Amundsen Sea and Ross Sea, where the seasonal variation of moisture flux is large.

Table 3 presents the annual mean *P-E* over Antarctica together with results of

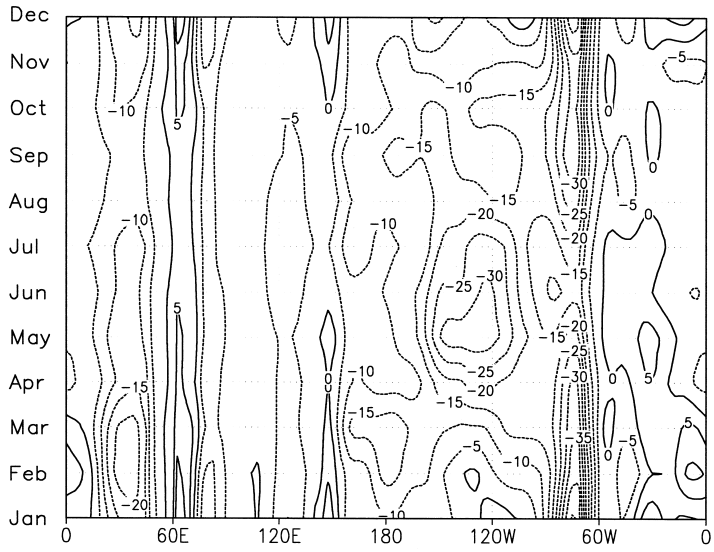

Fig. 11. Same as in Fig. 6 but for 67.5°S. The contour interval is 5 kg m^{-1} s^{-1}. Note that negative values indicate poleward flux.

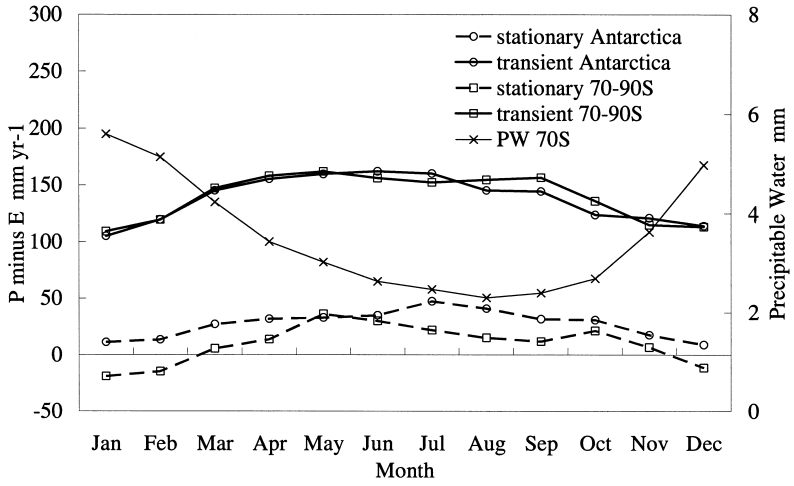

Fig. 12. Same as in Fig. 7 but for Antarctica.

previous studies. The values of *P-E* over both the Arctic and Antarctic regions in this study are reasonable. *P-E* from NCEP R2 is a little larger than that from ERA. This is consistent with the result of Cullather *et al.* (2000). In addition, we estimate *P-E* over the Antarctica region not including the Antarctic Peninsula. It is approximately 10 mm/year smaller than that over the Antarctica which is defined in this study (Fig. 1b). This suggests that *P-E* over Antarctica depends on the choice of the region, with

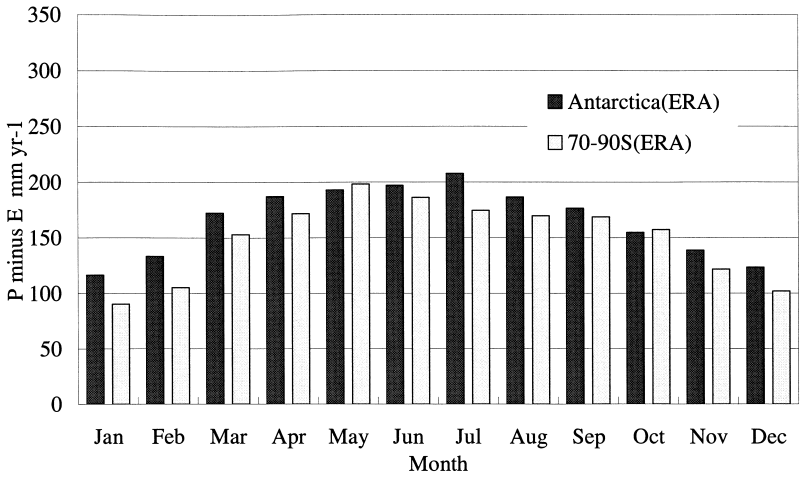

Fig. 13. Same as in Fig. 8 but for Antarctica.

Table 3. Same and in Table 2 but for Antarctica.

	Antarctica	70–90°S
Based on atmospheric data		
Peixoto and Oort, 1983 (Rawinsonde): 1963–1973	–	81
Yamazaki, 1992 (NMC): 1986–1990	135	162
Bromwich *et al*., 1995 (ECMWF): 1985–1992	157	140
Bromwich *et al*., 1995 (NMC): 1985–1992	108	134
Cullather *et al*., 1998 (ECMWF): 1985–1995	151	–
This study (ERA): 1979–1993	166	150
This study (NCEP R2): 1979–2002	112	160
Based on surface data		
Sellers (1965) multiyear	30	35
Baumgartner and Reichel (1975)	141	147
Giovinetto and Bull (1987)	143	–

a somewhat different result being particularly likely over the Antarctic Peninsula.

4. Interannual variation of moisture flux associated with annular modes

4.1. Arctic Oscillation

It is known that there is a relation between annular modes (AO and AAO) and moisture flux (Rogers *et al*., 2001; Boer *et al*., 2001). Figure 14a shows the correlation coefficient between the AO index and zonal mean moisture flux. The calculation is based on 15-year monthly mean data. In total, the sample size is 180. If the number of degrees of freedom is half of the sample size, *i.e*., 90, the significant level at 95% (99%) is 0.21 (0.27). For the zonal flux, the correlation has a maximum of 0.66 at 57.5°N and minimum of −0.53 at 27.5°–30°N. These correlations are quite significant

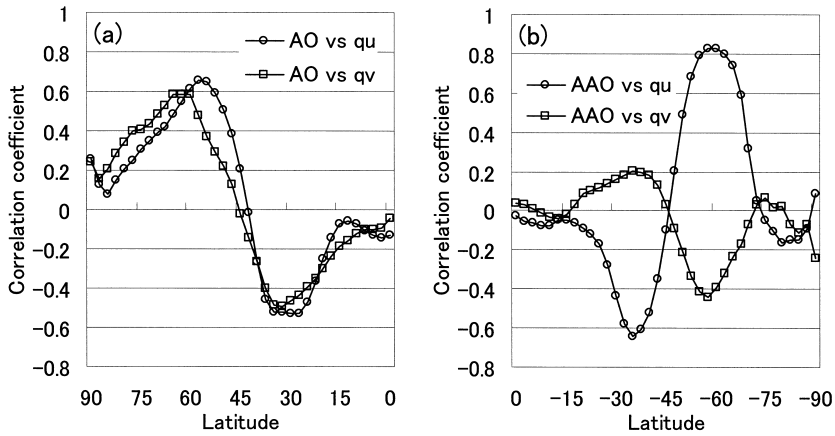

Fig. 14. (a) Correlation coefficients between the Arctic Oscillation (AO) index and zonal mean moisture flux for the zonal component (circles) and the meridional component (squares) in the Northern Hemisphere. Calculations are based on 15-year monthly mean data. In total, sample size is 180. When the number of degrees of freedom is half of the sample size, i.e., 90, the significant level at 95%(99%) is 0.21 (0.27). (b) The same as in (a) but for the Antarctic (AAO) index in the Southern Hemisphere.

and reasonable because the AO accompanies a similar zonal wind variation. For the meridional flux, the correlation shows a maximum of 0.59 at 60°–62.5°N and minimum of −0.49 at 32.5°–35°N. The meridional flux variation related to the AO is partly explained by the AO-related poleward wind variation in the lower troposphere. The variation of eddy moisture flux also contributes to this good correlation between the meridional moisture flux and the AO (Boer *et al*., 2001).

Figure 15a presents the AO regression pattern in the Northern Hemisphere. This is consistent with the fact that a positive polarity of AO is associated with a weakened Aleutian Low and intensified Icelandic Low. AO regression patterns for moisture flux over the Arctic are shown in Fig. 15b. A positive polarity of AO is related to enhanced poleward moisture flux from the Atlantic Ocean and cyclonic flux over the Arctic Ocean.

To indicate the seasonal change, Fig. 16 shows AO regression patterns for moisture flux for four seasons. Positive polarity of the AO is associated with an enhanced poleward moisture flux from the Atlantic Ocean in all seasons. It is also associated with an enhanced poleward flux in central Eurasia and an enhanced equator-ward flux though the Canadian Arctic Archipelago in boreal summer (JJA) and autumn (SON). The cyclonic flux over the Arctic Ocean is enhanced in boreal spring (MAM), summer and autumn. Especially in summer, these fluxes are enhanced. Note that the arrow scale in summer is three times larger than that in other maps in Fig. 16.

4.2. Antarctic Oscillation

Figure 14b shows the correlation coefficient between the AAO index and zonal mean moisture flux. They also have significant correlations. For the zonal flux, the

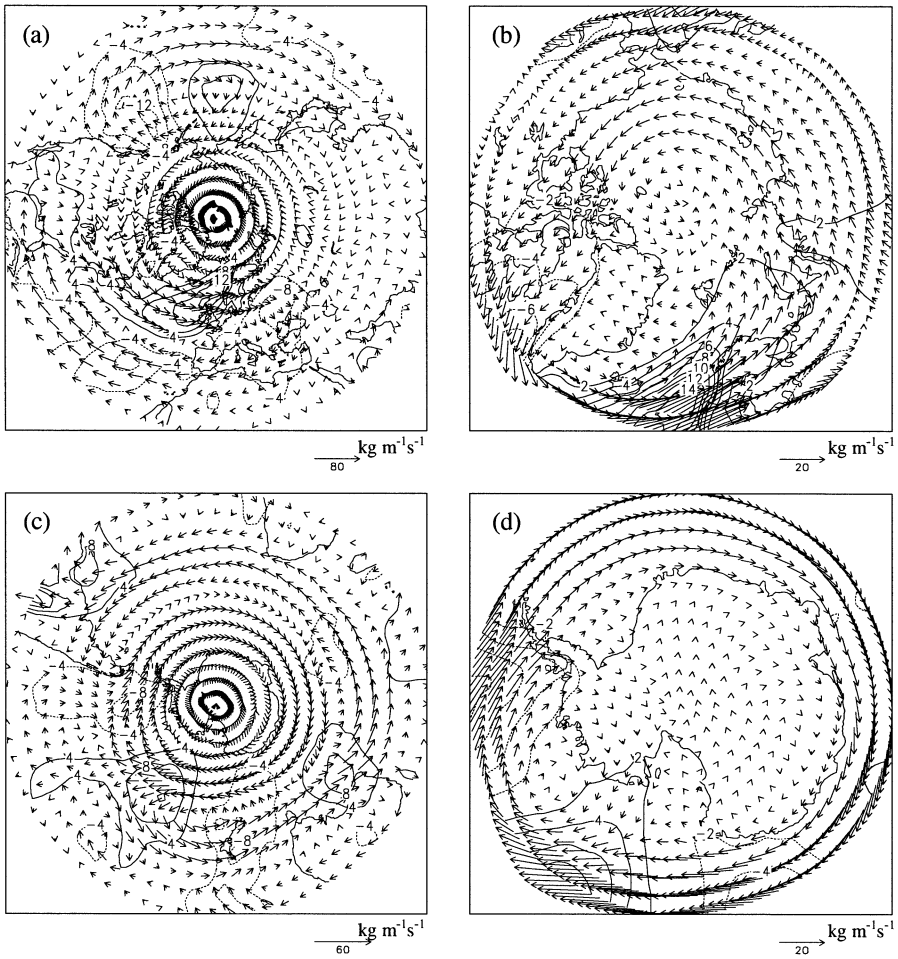

Fig. 15. (a) Moisture flux anomalies regressed onto the AO index in the Northern Hemisphere (poleward of 20°N). In the calculation, all the monthly mean data are used. (b) Same as in (a) but for the Arctic region. (c) Moisture flux anomalies regressed onto the AAO index in the Southern Hemisphere (poleward of 20°S). (d) Same as in (c) but for the Antarctic region. Vectors denote moisture flux anomalies and contours show their northward components. The arrow scale for moisture flux is shown at the bottom of each panel. Note that arrow scales are different among maps. The contour intervals in (a) and (c) are 4 kg m^{-1}s^{-1} and those in (b) and (d) are 2 kg m^{-1}s^{-1}.

correlation shows a maximum of 0.83 at 57.5°–60°S and minimum of −0.64 at 35°S. For the meridional flux, the correlation shows a maximum of 0.20 at 35°–37.5°S and minimum of −0.44 at 57.5°S. A similar discussion to that given for the AO can be applied to the AAO for the meridional flux. The correlation coefficient between meridional moisture flux and AAO becomes zero at 75°S and remains small poleward of 75°S. This indicates that the AAO is not associated with meridional flux in the interior

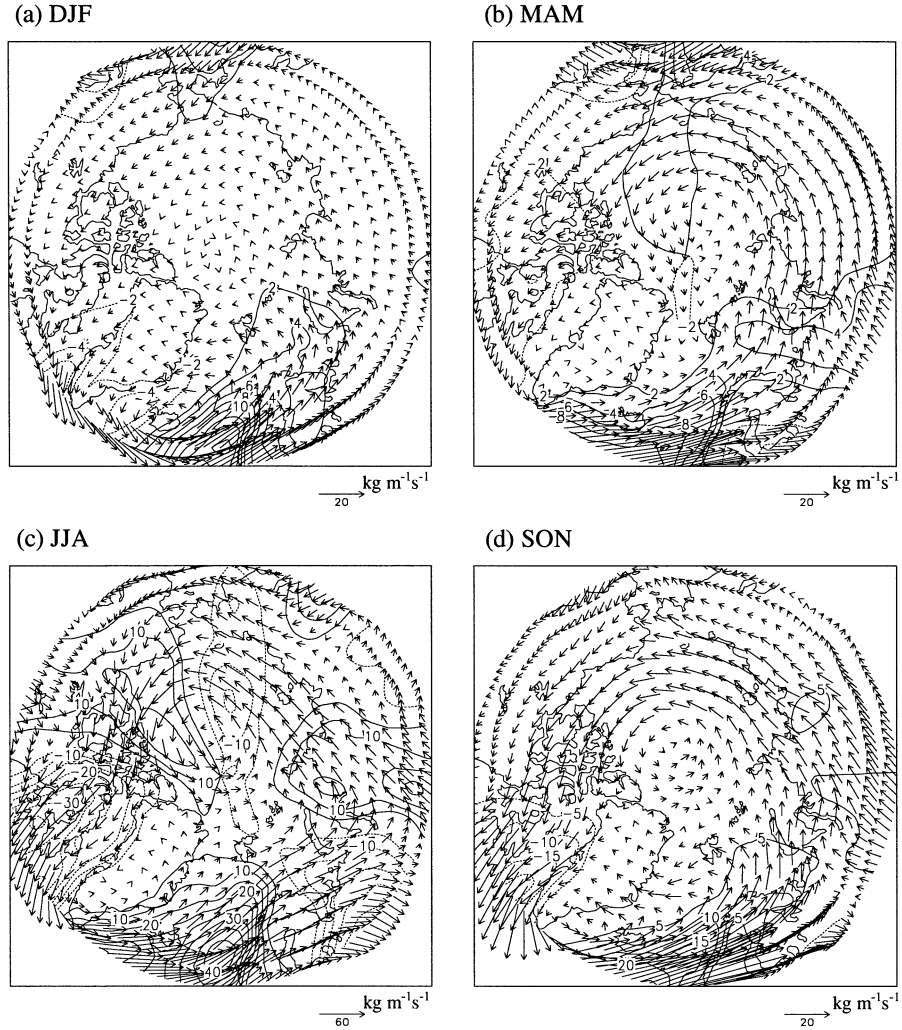

Fig. 16. Moisture flux anomalies regressed onto the AO index for four seasons. (a) Winter (December, January and February). (b) Spring (March, April and May). (c) Summer (June, July and August). (d) Autumn (September, October and November). Vectors denote moisture flux anomalies and contours show their northward components. The arrow scale for moisture flux is shown at the bottom of each panel. Note that the arrow scale in (c) is three times larger than those in other maps. The contour intervals in (a) and (b) are 2 kg $m^{-1}s^{-1}$*, and those in (c) and (d) are 5 kg* $m^{-1}s^{-1}$*. Calculations are based on 15-year monthly mean data for each season. In total, sample size is 45 for each season.*

of Antarctica. In contrast, the correlation coefficient at 75°N for the AO is 0.4 and the effect of the AO extends farther poleward compared with that of AAO.

The spatial pattern of moisture flux regressed on the AAO index is shown in Figs. 15c and 15d. Eastward transports are enhanced in high-latitudes (about 60°S) and

reduced in mid-latitudes (about 40°S). This is consistent with the lower-tropospheric wind anomalies related to the AAO. Furthermore, positive polarity of the AAO is related to cyclonic flux over the Bellingshausen Sea and the Amundsen Sea. The magnitude of moisture flux vector in the interior of Antarctica is very small. This corresponds to the low correlation coefficient poleward of 70°S (Fig. 14b).

Figure 17 shows moisture flux anomalies regressed onto the AAO index for four seasons. When the AAO is in a positive phase, eastward flux over the Antarctic Ocean

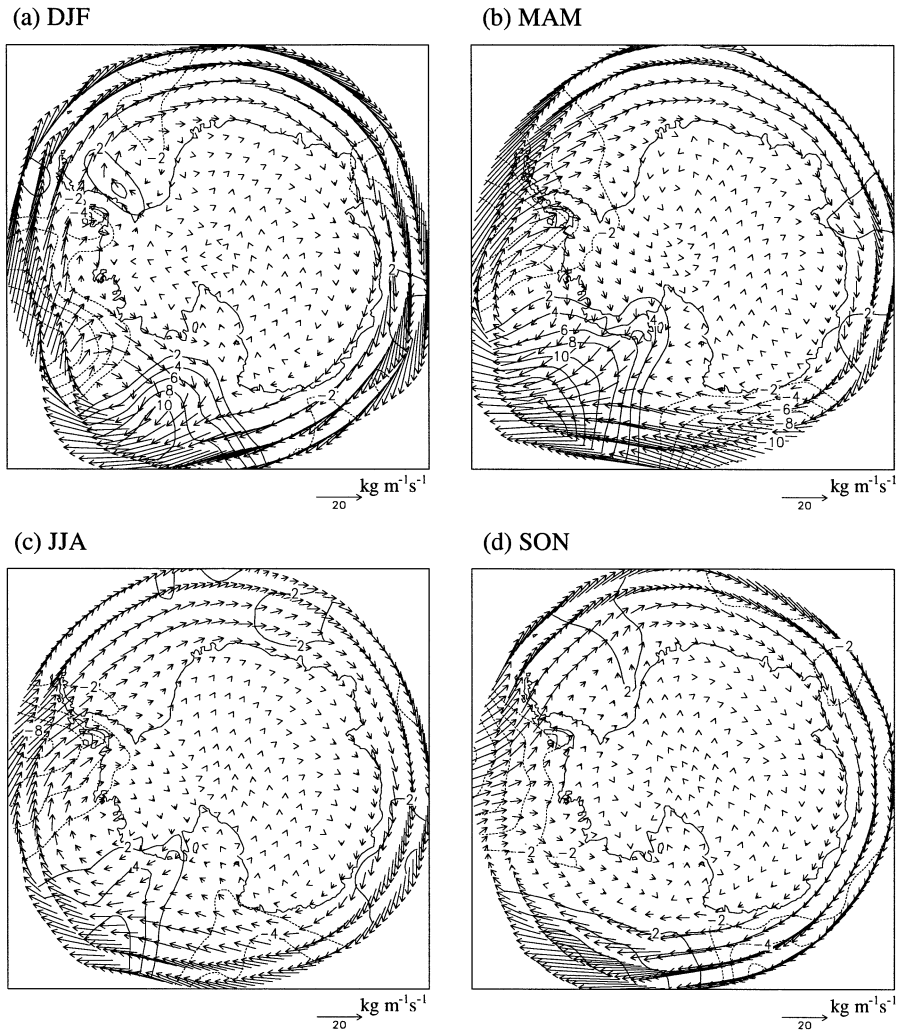

Fig. 17. Same as in Fig. 16 but for the AAO index. (a) Summer (December, January and February). (b) Autumn (March, April and May). (c) Winter (June, July and August). (d) Spring (September, October and November). Vectors denote moisture flux anomalies and contours show their northward components. The arrow scale for moisture flux is shown at the bottom of each panel. Contour interval is 2 kg m^{-1} s^{-1}.

surrounding Antarctica, and cyclonic flux over the Bellingshausen Sea and the Amundsen Sea, are enhanced. This cyclonic flux is enhanced especially in austral summer (DJF) and autumn (MAM). This is also consistent with the lower-tropospheric wind anomalies related to the AAO. Namely, a positive polarity of the AAO is related to deepened surface pressure over the Amundsen Sea.

5. Discussion and conclusions

We investigated the climatological seasonal variation of moisture transport over the Arctic and Antarctic regions and the interannual variations of moisture flux associated with annular modes, primarily using the 15-year ERA data set, and the NCEP R2 data set as a supplement.

Over the Arctic, there are strong moisture inflows from the Atlantic Ocean and Pacific Ocean in all seasons and strong outflow through the Canadian Arctic Archipelago in boreal summer. This inflow and outflow are especially enhanced in boreal summer due to the summer moisture increase. We divided the total moisture flux into stationary and transient components. The transient moisture flux is poleward at all longitudes and enhanced in boreal summer. In particular, summer poleward flow from central Eurasia is caused by transient moisture transport. The seasonal variation of moisture inflow into the Arctic is controlled mainly by transient flux, which shows a boreal summer maximum due to large precipitable water in boreal summer. Therefore, *P-E* over the Arctic exhibits a summer maximum.

Over the Antarctic, a strong moisture inflow exists west of the Antarctic Peninsula in all seasons and over the Bellingshausen Sea and the Amundsen Sea in austral autumn and winter. Most moisture inflows to Antarctica have maxima in austral summer and minima in winter, but the inflows over the Bellingshausen Sea and the Amundsen Sea have maxima in winter and minima in austral summer. As a result, the seasonal variation of *P-E* over the Antarctic shows an austral winter maximum, which is opposite to that over the Arctic. Geographically, the moisture inflow over the Bellingshausen Sea and the Amundsen Sea contributes to this peculiar seasonal variation. When moisture flux is divided into stationary and transient components, both components show a winter maximum, even though *PW* shows a summer maximum.

Transient flux greatly contributes to *P-E* in both the Arctic and Antarctic regions. Therefore, the seasonal variations of *P-E* over these regions are mainly explained by the effect of poleward transient moisture flux, although stationary flux is comparable in the Antarctic region. Over the Arctic, the seasonal variation of poleward transient moisture flux primarily depends on the seasonal variation of *PW* and that over the Antarctic primarily depends on cyclone activity.

The annual mean (*P-E*)s over the Arctic Ocean and Antarctica are 186 mm/year and 166 mm/year, respectively. This annual mean *P-E* over the Arctic Ocean is equivalent to 55×10^{-3} Sv ($1\,\mathrm{Sv} = 10^6\,\mathrm{m^3\,s^{-1}}$, this unit is commonly used in oceanography). The river runoff into the Arctic Ocean is $112\text{–}136 \times 10^{-3}$ Sv. The sum of river runoff and *P-E*, 0.167–0.191 Sv, is the total input of fresh water into the Arctic Ocean. Thus two thirds of fresh water input to the Arctic Ocean comes from river runoff and one third from the atmosphere.

The Arctic Oscillation (AO) and zonal mean meridional moisture flux have a significant positive correlation. The maximum correlation of 0.59 is found at 60°–62.5°N. The Antarctic Oscillation (AAO) has the same relation to the poleward moisture flux. The maximum correlation of −0.44 is found at 57.5°S. These results agree with previous studies (Boer *et al*., 2001; Roger *et al*., 2001). It is also found that the AAO is not associated with meridional flux in the interior of Antarctica.

Positive polarity of the AO is associated with a poleward moisture flux anomaly from the Atlantic Ocean throughout the year, cyclonic flux in boreal spring, summer and autumn, and equator-ward flux through the Canadian Arctic Archipelago in boreal summer and autumn. Positive polarity of the AAO is associated with eastward moisture flux over the Antarctic Ocean surrounding Antarctica and cyclonic flux over the Bellingshausen Sea and the Amundsen Sea, especially in austral summer and autumn. Although, in austral summer, westward moisture flux along the coastline of East Antarctica exists in the annual mean flux field, positive polarity of the AAO is associated with eastward flux anomalies along the coastline. Therefore, moisture flux anomalies over both the Arctic and the Antarctic related to the annular modes correspond to lower-tropospheric wind anomalies. This is because moisture is abundant in the lower troposphere.

The results from NCEP R2 are almost the same as those from ERA. Our results are consistent with those of Bromwich *et al*. (2000) and Bromwich *et al*. (1995), who used ERA, ECMWF, NCEP-NCAR or NMC, though the version is different. It is considered that these differences are caused by differences in performance and horizontal resolutions of the models.

These estimations of the atmospheric moisture budget and clarification of the relations between annular modes and moisture transports are helpful to assess the water cycle over the entire polar regions and its interannual variations.

Acknowledgments

The authors benefited from useful comments given at the 26th NIPR Symposium on Polar Meteorology and Glaciology at NIPR, Tokyo in 2003. We also thank two anonymous reviewers for comments on the original manuscript. NCEP-DOE Reanalysis-2 data were provided by the NOAA-CIRES Climate Diagnostics Center, Boulder, Colorado, USA, *via* their Web site at http: //www.cdc.noaa.gov/. The GFD DENNOU Library and GrADS were used for analysis and drawing figures.

References

Baumgarner, A. and Reichel, E. (1975): The World Water Balance. Elsevier, 179 p.

Boer, G.J., Fourest, S. and Yu, B. (2001): The signature of the annular modes in the moisture budget. J. Climate, **14**, 3655–3665.

Bromwich, D.H., Robasky, F.M., Cullather, R.I. and Van Woert, M.L. (1995): The atmospheric hydrologic cycle over the Southern Ocean and Antarctica from operational numerical analyses. Mon. Weather Rev., **123**, 3518–3538.

Bromwich, D.H., Cullather, R.I. and Serreze, M.C. (2000): Reanalyses depictions of the Arctic atmospheric moisture budget. The Fresh Water Budget of the Arctic Ocean, ed. by E.L. Lewis. Kluwer, 163–196.

Cullather, R.I., Bromwich, D.H. and Van Woert, M.L. (1998): Spatial and temporal variability of Antarctic precipitation from atmospheric methods. J. Climate, **11**, 334–367.

Cullather, R.I., Bromwich, D.H. and Serreze, M.C. (2000): The atmospheric hydrologic cycle over the Arctic basin from reanalyses. Part I: Comparison with observations and previous studies. J. Climate, **13**, 923–937.

Giovinetto, M.B. and Bull, C. (1987): Summary and analyses of surface mass balance compilations for Antarctica, 1960–1985. Byrd Polar Res. Center Rep., **1**, 90 p.

Gong, D. and Wang, S. (1999): Definition of Antarctic Oscillation index. Geophys. Res. Lett., **26**, 459–462.

Groves, D.G. and Francis, J.A. (2002a): Moisture budget of the Arctic atmosphere from TOVS satellite data. J. Geophys. Res., **107**(D19), 4391, doi: 10.1029/2001JD001191.

Groves, D.G. and Francis, J.A. (2002b): Variability of the Arctic atmospheric moisture budget from TOVS satellite data. J. Geophys. Res., **107**(D24), 4785, doi: 10.1029/2002JD002285.

Peixoto, J.P. and Oort, A.H. (1983): The atmospheric branch of the hydrological cycle and climate. Variations in the Global Water Budget, ed. by A. Street-Perrott *et al*. D. Reidel, 5–65.

Peixoto, J.P. and Oort, A.H. (1992): Physics of Climate. American Institute of Physics, 520 p.

Rogers, A.N., Bromwich, D.H., Sinclair, E.N. and Cullather, R.I. (2001): The atmospheric hydrologic cycle over the Arctic basin from reanalyses. Part II: Interannual variability. J. Climate, **14**, 2414–2429.

Sellers, W.D. (1965): Physical Climatology. University of Chicago Press, 272 p.

Serreze, M.C. and Barry, R.G. (2000): Atmospheric components of the Arctic Ocean hydrologic budget assessed from rawinsonde data. The Fresh Water Budget of the Arctic Ocean, ed. by E.L. Lewis. Kluwer, 141–161.

Serreze, M.C., Barry, R.G. and Walsh, J.E. (1995): Atmospheric water vapor characteristics at 70°N. J. Climate, **8**, 719–731.

Thompson, D.W.J. and Wallace, J.M. (1998): The Arctic Oscillation signature in the wintertime geopotential height and temperature fields. Geophys. Res. Lett., **25**, 1297–1300.

Thompson, D.W.J. and Wallace, J.M. (2000): Annular modes in the extratropical circulation. Part I: Month-to-month variability. J. Climate, **13**, 1000–1016.

Yamazaki, K. (1992): Moisture budget in the Antarctic atmosphere. Proc. NIPR Symp. Polar Meteorol. Glaciol., **6**, 36–45.

Yamazaki, K. (1994): Moisture budget in the Antarctic atmosphere. Snow and Ice Covers: Interactions with the Atmosphere and Ecosystems, ed. by H.G. Jones *et al*. Wallingford, IAHS, 61–67 (IAHS Publ., **223**).

Yamazaki, K. (1997): Seasonal variation of atmospheric water circulation in the Antarctic region derived from objective analysis data. Nankyoku Shiryô (Antarct. Rec.), **41**, 149–160.